Penerbit
Akademia Baru

Modelling of Convective Heat Transfer of Nanofluid in Inversed L-Shaped Cavities

N. A. Che Sidik[*] and A. Safdari

Faculty of Mechanical Engineering, Universiti Teknologi Malaysia, 81310 Johor, Malaysia.
*azwadi@mail.fkm.utm.my

Abstract – *Research on nanofluids has been quite intensive in the past decade. Whilst there have been many studies analyzing the performance of nanofluids, the behavior of nanofluid confined in complicated geometry, especially those using numerical simulation, are scarce. In this study, the behaviors of nanofluid in inverse L-shaped of cavity were simulated using in-house matlab code. The cubic interpolated pseudo particle method was used to solve the governing equation of nanofluid. The results showed improvements in terms heat transfer with the presence of nanofluid and the nanoparticle volume fraction significantly increase the Nusselt number in the enclosure. Analyses on the aspect ratio, Rayleigh number, nanoparticle volume fraction and thermal conductivity of nanofluid showed their significant effect on the performance of the nanofluid confined in inverse L-shaped of cavity.* ***Copyright © 2016 Penerbit Akademia Baru - All rights reserved.***

Keywords: Nanofluid, Volume fraction, Nusselt number, Rayleigh number, Numerical method

1.0 INTRODUCTION

The natural convection heat transfer is one of the classical heat transfer problems that can narrate the development of modern understanding of heat transfer. Literature records include research on such problem since 1969 [1] until today [2-4]. On the other hand, the natural convection heat transfer in enclosure has been extensively used to analyze the physics of the flow or as a benchmark for new numerical scheme. In addition, the natural convection in enclosure has been notable importance to several engineering applications, such as cooling of electronic equipment, nuclear and chemical reactors, thermal storage system, etc. The vast majority of these researches have considered square or rectangular enclosure, with different aspect ratios. The natural convection in enclosure is generally characterized by the vortices stimulated by the buoyancy force. Lo et al. [5] have recently conducted remarkable effort to thoroughly describe the vortex behavior of natural convection in enclosure at wide range of Rayleigh numbers.

As a matter of fact, real engineering applications involve many different kind of enclosures such as arc-shaped enclosure, wavy enclosure, eccentric elliptical enclosure, etc. Chen and Cheng [6] dedicated their study on the flow and heat transfer characteristic inside an arc-shape of enclosure at various orientations. Saidi et al. [7] and Shohel et al. [8] focused on the vortex structure analysis in a vertical wavy wall and its effect on the rate of heat exchange between the wavy wall and the flowing fluid. The flow pattern and heat transfer characteristic in an L-shaped enclosure has been a topic of study by Tasnim and Mahmud [9], Angirasa and Mahajan [10] and Chinnakotla et al. [11]. Recently, Mahmoodi [12] extended the research by replacing

the medium with a nanofluid for the purpose to increase the rate of heat transfer in an L-shaped enclosure.

Recently, the natural convection of nanofluid was widely studied because of its importance in industrial applications such as heat exchanger, solar energy collector, chemical vapor deposition instrument, etc. A number of researches have been conducted dealing with different kinds of nanoparticles to investigate nanofluid effectiveness on heat transfer and fluid flow.

Experimental studies on the natural convection of nanofluid in a vertical square enclosure of different sizes have been conducted by Ho et al. [13] and the same configuration was examined numerically by Shahi et al. [14]. Detailed discussion of the natural convection of nanofluid can be found in literatures such as Hakan and Abu-Nada [15-16], Mahmoodi [17], Mahmoodi and Seyed [18] and many more [19-21]. A quick review of these works shows that the efficiency of heat transfer by nanofluid is significantly affected by the geometry of the system and the choice of suspended nanoparticle.

The numerical works on natural convection of nanofluid in an enclosure have been conducted by many researchers. Khanafer et al. [22] initiated the numerical research to determine the effect of solid volume fraction on the rate of heat transfer in a square enclosure. Similar attempts have been carried out by Kefayati [23] using an alternative numerical method of lattice Boltzmann. The results of these researches show that the presence of nanoparticles alters the flow structure and increases the rate of heat transfer. This trend was confirmed by Parametthanuwat et al. [24], Khwanchit and Smith [25] and Ghadimi [26]. The authors also concluded that the suspended particle density and solid volume fraction play significant role in enhancing the rate of heat transfer of nanofluid.

In the present investigation, the natural convection of nanofluid in inverse L-shaped of enclosure is visited. The main aim of the present study is to further investigate the effects of the dimensionless parameter of Rayleigh number, the aspect ratio of inverse L-shaped of cavity, the solid volume fraction of nanoparticles and different types of nanoparticle suspended in water on the flow and heat transfer characteristics inside the enclosure. The cavity is filled with five different water based Cu, SiO_2, CuO, Al_2O_3 or TiO_2 nanoparticles. The results will be presented in terms of streamlines, isotherms and average Nusselt number.

The paper is organized as follows: in the next section the mathematical formulation and numerical model are given, in the third section, the grid dependency and validation tests are reported. Then the numerical results and analyses concerning the parametrical study for the natural convection of nanofluid in inverse L-shaped of enclosure are presented in the section four. Finally, section five concludes the current study.

2.0 PROBLEM PHYSICS AND RESEARCH METHODOLOGY

Figure 1 shows a two-dimensional inverse L-shaped of cavity with height and width are noted by H and W respectively. Here we define the aspect ratio as AR = L/H. The cavity is filled with a suspension of Cu, SiO2, CuO, Al2O3 or TiO2 nanoparticles and water. The thermophysical properties of the nanoparticle and water at reference temperature are presented in Table 1.
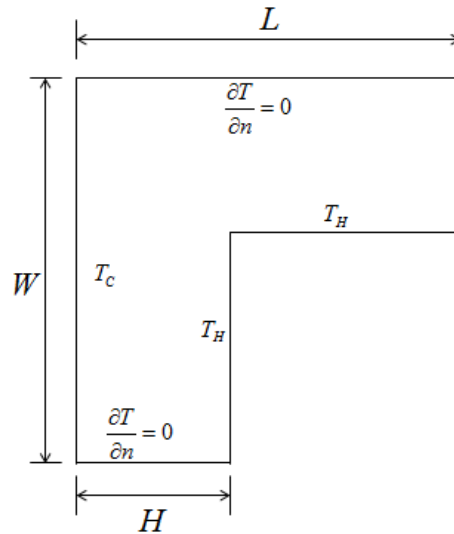
Figure 1: Schematic diagram of inversed L-shaped of cavity.

Table 1: Physical property of nanoparticles and water

Physical Properties	Cu	SiO$_2$	CuO	Al$_2$O$_3$	TiO$_2$	Water
c$_p$ (J/Kg K)		383	765	540	765	686.2	4179
ρ (kg/m3)		8954	3970	6500	3970	4250	997.1
K (W/m K)		400	36	18	25	8.95	0.613
β × 10^5 (K^{-1})	1.67	0.63	0.85	0.85	0.9	21	

In the present study, the left and right vertical walls are kept at two different temperatures to induce the buoyancy effect in the enclosure. Here, the Boussinesq approximation is applied where the density in the buoyancy force is assumed has a linear relation with temperature. However, the rest of thermophysical properties are presumed to be constant [26]. It is further assumed that the nanoparticle and the based fluid are in thermal equilibrium. The governing equations for laminar, incompressible, transient and Newtonian nanofluids are expressed as follow

The vorticity transport equation:

$$\frac{\partial \omega}{\partial t} + \frac{\partial}{\partial x}\left(\omega \frac{\partial \psi}{\partial y}\right) - \frac{\partial}{\partial y}\left(\omega \frac{\partial \psi}{\partial x}\right) = \frac{\mu_{nf}}{\rho_{nf}}\left(\frac{\partial \omega}{\partial x^2} + \frac{\partial \omega}{\partial y^2}\right) + \frac{\left(\varphi \rho_s \beta_s + (1-\varphi)\rho_f \beta_f\right)}{\rho_{nf}} g\left(\frac{\partial T}{\partial x}\right) \qquad (1)$$

The energy transport equation:

$$\frac{\partial T}{\partial t} + \frac{\partial}{\partial x}\left(T\frac{\partial \psi}{\partial y}\right) - \frac{\partial}{\partial y}\left(T\frac{\partial \psi}{\partial x}\right) = \frac{\partial}{\partial x}\left(\alpha_{nf}\frac{\partial T}{\partial x}\right) + \frac{\partial}{\partial y}\left(\alpha_{nf}\frac{\partial T}{\partial y}\right) \tag{2}$$

and the vorticity equations:

$$\omega = -\left(\frac{\partial^2 \psi}{\partial x^2} + \frac{\partial^2 \psi}{\partial y^2}\right) \tag{3}$$

where the thermal diffusivity is expressed as

$$\alpha_{nf} = \frac{k_{nf}}{(\rho c_p)_{nf}} \tag{4}$$

The effective density of a fluid containing suspended particles at a reference temperature is given by

$$\rho_{nf} = (1-\varphi)\rho_f + \varphi\rho_s \tag{5}$$

where φ, ρ_f and ρ_s are the volume fraction of suspended particles, particles density and density of based fluid, respectively. The effective viscosity for nanofluid which is consist of pure water with viscosity μ_f and a dilute suspension of small solid spherical particles is given by Brinkman [27] as

$$\mu_{nf} = \frac{\mu_f}{(1-\varphi)^{2.5}} \tag{6}$$

The heat capacitance of the nanofluid can be written as

$$(\rho c_p) = (1-\varphi)(\rho c_p)_f + \varphi(\rho c_p)_s \tag{7}$$

The effective stagnant thermal conductivity of the solid–liquid mixture was first developed by Wasp [28] as and will be applied in the present study

$$\frac{k_{nf}}{k_f} = \frac{k_s + 2k_f - 2\varphi(k_f - k_s)}{k_s + 2k_f + \varphi(k_f - k_s)} \tag{8}$$

This equation can be applied for a two-phase combination, containing microscopic solid particles. Without suitable equation for computation of thermal conductivity behavior, the solid–liquid mixture, Eq. (8) can be roughly used to extract a logical approximation.

In order to have independent results from the scale of the system, the following dimensionless variables will be used on the equation

$$\Psi = \frac{\psi}{\sqrt{g\beta_f \Delta T H^3}} \quad , \quad \Omega = \frac{\omega H^2}{\sqrt{g\beta_f \Delta T H^3}}$$

$$X = \frac{x}{H} \quad , \quad Y = \frac{y}{H} \tag{9}$$

$$\tau = \frac{t\sqrt{g\beta_f \Delta T H^3}}{H} \quad , \quad U = \frac{u}{\sqrt{g\beta_f \Delta T H^3}} \quad , \quad V = \frac{v}{\sqrt{g\beta_f \Delta T H^3}}$$

$$\theta = \frac{T - T_C}{T_H - T_C}$$

In order to apply above dimensionless variables to the governing equations of (1) and (2), we consider the dimensionless form of the vorticity and energy equations which can be presented in the general form of differential equation as follows

$$\varepsilon_\sigma \frac{\partial \sigma}{\partial \tau} + \frac{\partial}{\partial X}\left[U\sigma - \Gamma_\sigma \frac{\partial \sigma}{\partial X} \right] + \frac{\partial}{\partial Y}\left[V\sigma - \Gamma_\sigma \frac{\partial \sigma}{\partial X} \right] = \eta_\sigma \tag{10}$$

where σ stands for either Ω or θ with

$$\varepsilon_\theta = 1,$$

$$\Gamma_\theta = \frac{1}{\Pr \sqrt{Gr}} \frac{k_{nf}}{k_f}\left[(1-\varphi) + \varphi \frac{(\rho c_p)_s}{(\rho c_p)_f} \right]^{-1}$$

$$\eta_\theta = \frac{1}{\Pr \sqrt{Gr}}\left[\frac{\partial(\Gamma_\theta \Pr \sqrt{Gr})}{\partial X}\frac{\partial \theta}{\partial X} + \frac{\partial(\Gamma_\theta \Pr \sqrt{Gr})}{\partial Y}\frac{\partial \theta}{\partial Y} \right] \tag{11}$$

$$\varepsilon_\Omega = 1,$$

$$\Gamma_\Omega = \left[(1-\varphi)^{2.5}\left[\varphi \frac{\rho_s}{\rho_f} + (1-\varphi) \right]\sqrt{Gr} \right]^{-1}$$

$$\eta_\Omega = \Lambda \frac{\partial \theta}{\partial X} \tag{12}$$

where Prandtl Number, $\Pr = \frac{v_f}{\alpha_f}$, Grasshof Number, $Gr = \frac{\beta_f g(T_H - T_C)H^3}{v_f^2}$ and

$$\Lambda = \left[\left(1 - \frac{(1-\varphi)}{\varphi}\frac{\rho_f}{\rho_s} \right)^{-1}\frac{\beta_s}{\beta_f} + \left(1 + \frac{\varphi}{(1-\varphi)}\frac{\rho_s}{\rho_f} \right)^{-1} \right] \tag{13}$$

The cubic interpolated pseudo particle method (CIP) was used to solve the above governing equation. Details formulation of CIP method can be seen in ref. [29-31].

3.0 GRID INDEPENCY TEST

Before the prediction is started, a grid dependency test was carried out to determine a proper grid size for the simulation. Seven different mesh sizes namely 30^2, 40^2, 50^2, 60^2 and 70^2, 80^2 and 90^2 were employed for prediction at Ra = 10^6, Cu-water based nanofluid, aspect ratio 0.4 and 10% of volume fraction. Table 2 shows the calculated average Nusselt number in the system. As can be seen from the table, a 70^2 grid is sufficiently fine to meet the requirement of computational time and grid independent solution. Based on this result, a grid size of 70^2 was used in all calculations.

Table 2: Grid dependency test for Cu-water based nanofluid, AR = 0.4 and 10% of volume fraction

Grid Size	30^2	40^2	50^2	60^2	70^2	80^2	90^2
Nusselt No.	15.177	16.042	16.683	17.257	17.541	17.765	17.927

4.0 SIMULATION RESULTS AND DISCUSSION

Effect of Rayleigh number: We firstly analyze the case for solid volume fraction 5% of Al_2O_3-water based nanofluid. Figures 2 and 3 show the plots of streamlines and isotherms for variations of Rayliegh numbers.

(a)   (b)

(c)   (d)
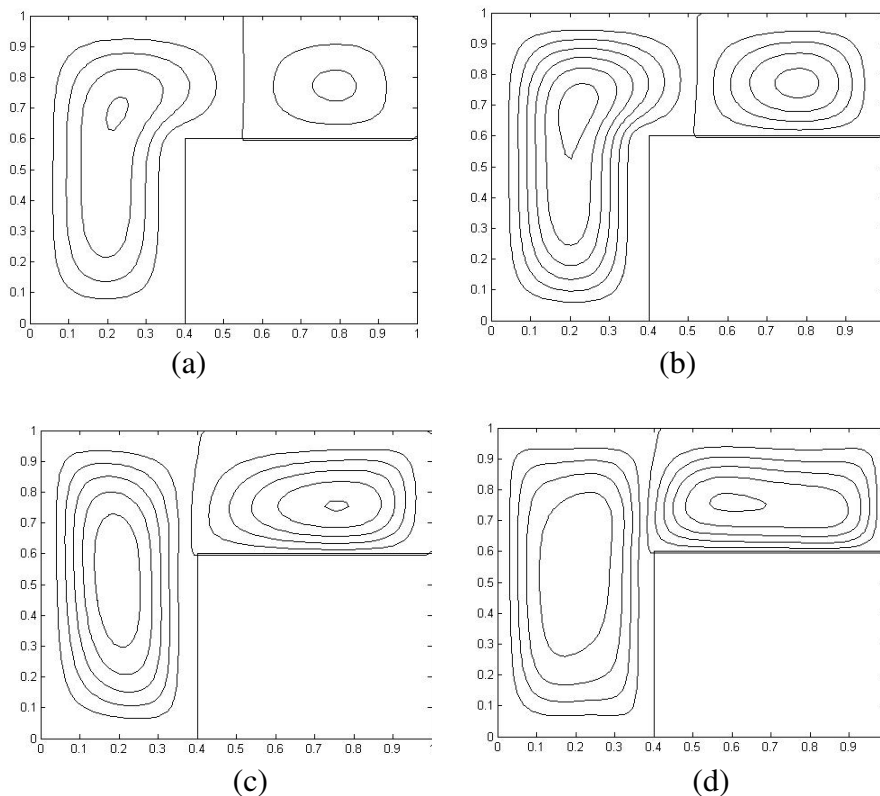
Figure 2: Variations of streamline in inverse L-shaped of cavity at Rayleigh number (a)10^3, (b)10^4, (c) 10^5 and (d)10^6

(a)   (b)

(c)   (d)
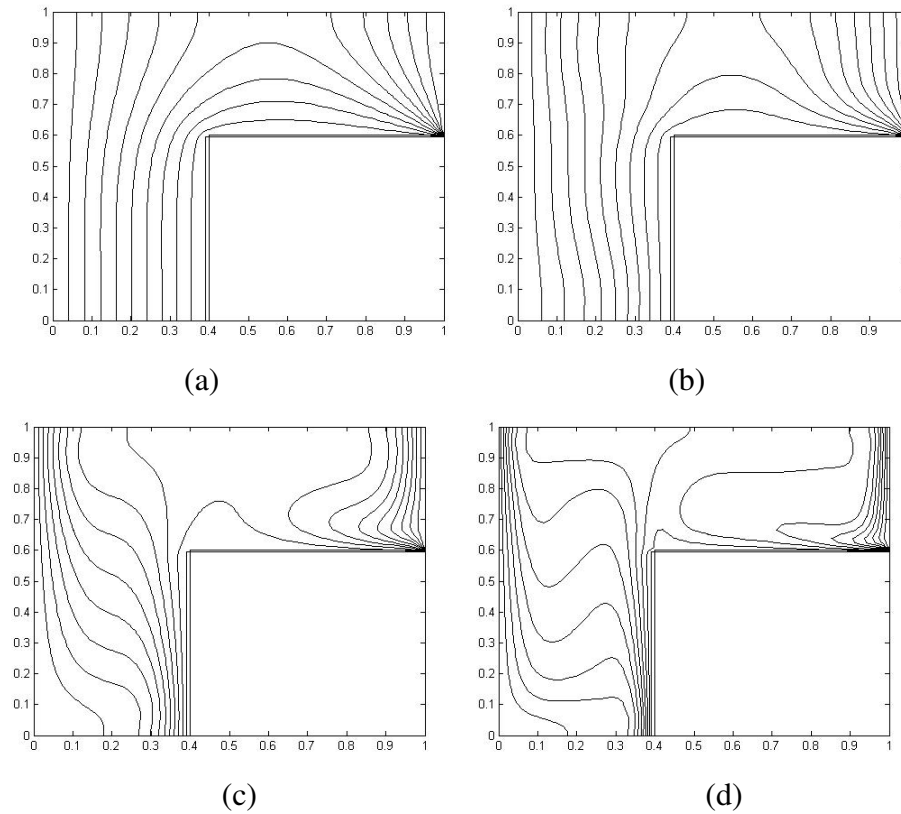
Figure 3: Variations of isotherms in inverse L-shaped of cavity at Rayleigh number
(a)10^3, (b)10^4, (c) 10^5 and (d)10^6

The streamline in Figure 2a and 2b show that a single vortex is developed inside the vertical and horizontal regions of the cavity. This counter-clockwise direction of vortex brings the hot air to the top cavity then cooled by the cold left wall. This weak vortex is observed not capable to contribute to the enhancement of heat transfer and therefore, the main heat transfer mechanism at this Rayleigh numbers (Ra = 10^3 and 10^4) is by conduction. While the vortex in the top horizontal cavity is increasing its size, the shape of isotherms is gradually distorted as the Rayleigh number is increased. Distinct thermal boundary layer can be seen adjacent to the vertical isothermal walls indicates the convective mode of heat transfer mechanism.

Effect of Aspect Ratio on Average Nusselt Number: Next we analyze the value of average Nusselt number along the hot walls of inverse L-shaped cavity. Table 3 shows the computed results for variations of aspect ratio, Rayleigh number and volume fraction of nanofluid SiO_2-water. Table shows that for Ar = 0.2, the computed average Nusselt number is almost similar for all range of Rayleigh number. It means that the conduction mode of heat transfer is the dominant heat transfer mechanism. For the computation at Ar = 0.4, small increment of Nusselt number when Rayleigh number increase from 10^3 to 10^4. Then the Nusselt number increase significantly at Ra = 10^5 indicates convective heat transfer mechanism takes place. Finally at Ar = 0.6, gradual increment of Nusselt number when the Ra increase demonstrating heat transfer mode from conduction to convection.

Table 3: Variations of average Nusselt number with different Rayleigh numbers, aspect ratio and volume fraction.

| Rayleigh Number	Volume fraction	Ar = 0.2	Ar = 0.3	Ar = 0.4
10^3	0%	5.069	4.582	4.646
	1%	5.212	4.712	4.778
	3%	5.506	4.980	5.051
	5%	5.813	5.260	5.335
	10%	6.639	6.011	6.099
10^4	0%	5.069	4.562	4.949
	1%	5.212	4.689	5.070
	3%	5.506	5.025	5.317
	5%	5.812	5.299	5.575
	10%	6.636	6.019	6.276
10^5	0%	5.397	6.367	8.102
	1%	5.535	6.485	8.261
	3%	5.790	6.720	8.575
	5%	6.033	6.953	8.885
	10%	6.717	7.543	9.639
10^6	0%	8.967	11.431	13.899
	1%	9.099	11.665	14.192
	3%	9.416	12.116	14.391
	5%	9.723	12.563	14.928
	10%	10.450	13.654	16.269

Effect of Volume Fraction: To highlight the influence of variation of the volume fraction of nanoparticle on the Nusselt number, the volume fraction was varied from 0% to 10% for three different cavity aspect ratios. In this case, the CuO nanofluid was chosen as test fluid. For AR = 0.2, we can see from Fig. 4 that there is significant effect of the presence of nanoparticle on the calculated average Nusselt number in the cavity of inverse L-shaped enclosure. The addition of nanoparticles stimulates the flow, reduce the thermal boundary layer thickness and hence increase the Nusselt number. However, even the Rayleigh number is increase to 10^5, there is very small augmentation in the value of average Nusselt number. For example, at φ = 0.05, increment of Rayleigh number from 10^3 to 10^5, the average Nusselt number increases only about 1.5%.

Figures 5 and 6 demonstrate the obtained results for aspect ratio of 0.4 and 0.6. These figures show that the effect of volume fraction becomes less and less as the aspect ratio increases. This can be seen from the gap between the three lines becomes closer and closer at higher aspect ratio. Moreover, it is evident that the effect of volume fraction on average Nusselt number enhancement is more at high Rayleigh number for a fixed aspect ratio of Ar = 0.6.

Effect of Types of Nanofluid: The current investigation is wrapped with the analysis of the effect of types of nanofluid on the heat transfer enhancement in the cavity. Figures 7 and 8 display values of average Nusselt number at various Rayleigh numbers, aspect ratio 0.3 and solid volume fraction of 1% and 10% respectively. These figures demonstrate that the Nusselt number increases with the Rayleigh number for all types of nanofluid tested in the present study. High Rayleigh number results in high energy transport through the fluid and cause irregular motion of nanoparticle. The higher solid volume fraction further stimulates the flow and contributes to higher Nusselt number as shown in the figures. The presence of nanoparticles also increases the rate of heat transfer by conduction mode through the flow. It is the main reason the figure demonstrates that the highest thermal conductivity of Cu nanoparticles gives the highest average Nusselt number for all simulation conditions.
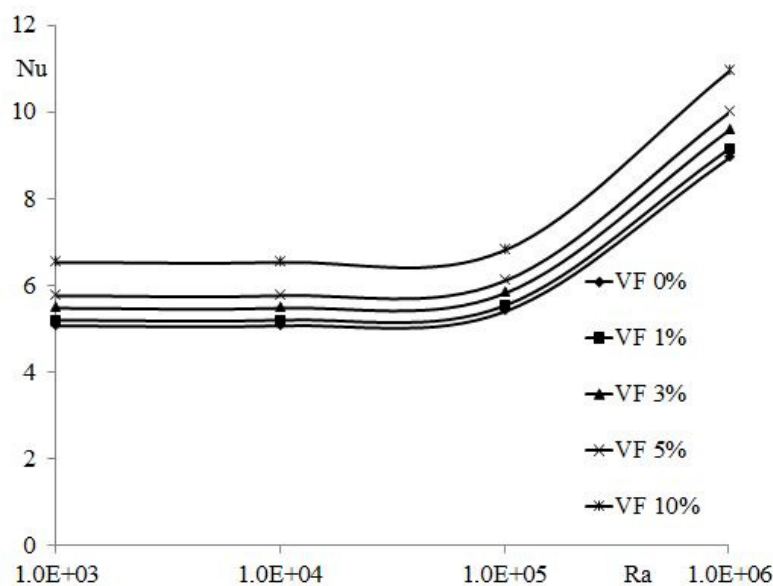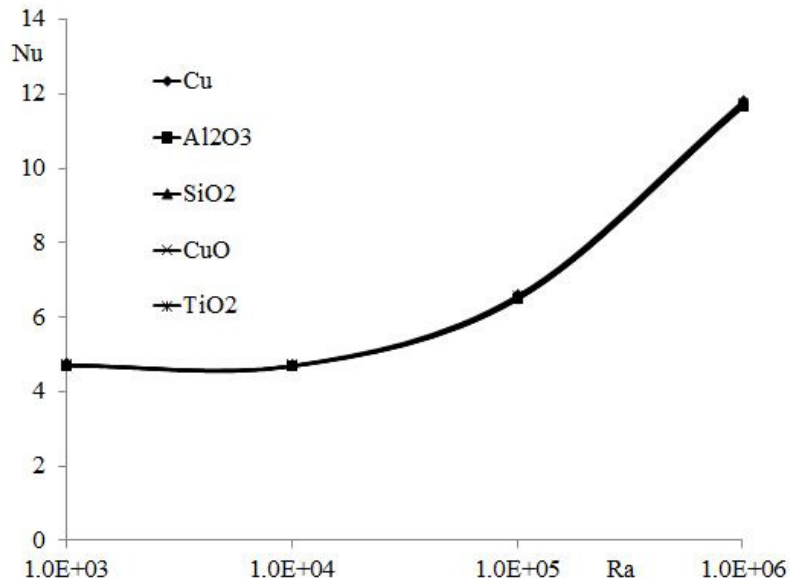

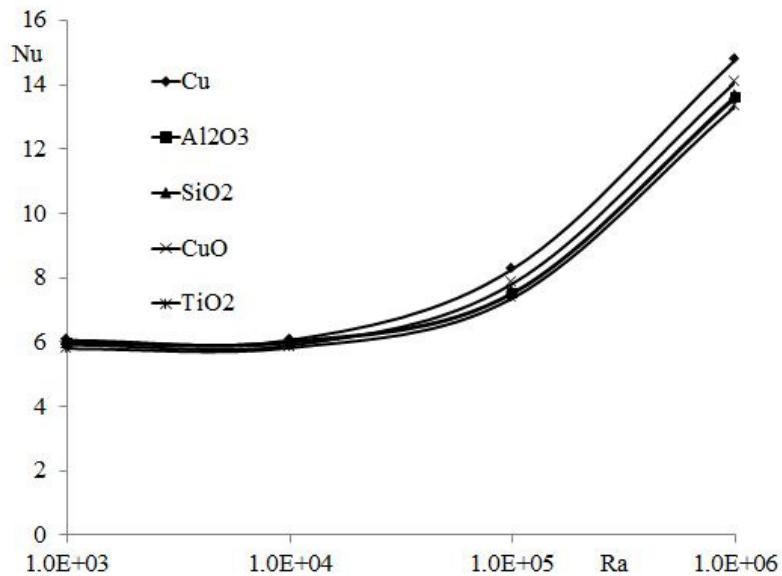**Figure 4:** Average Nusselt number in inverse L-shaped of cavity for AR = 0.2.
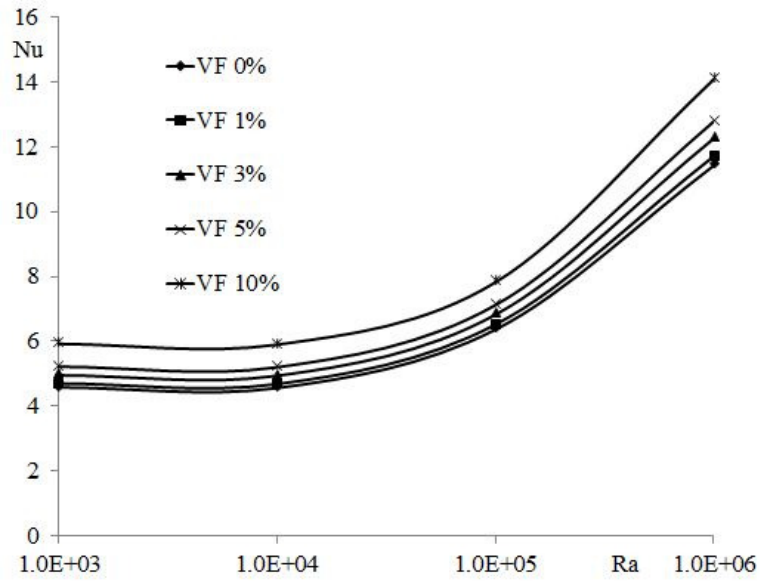
Figure 5: Average Nusselt number in inverse L-shaped of cavity for AR = 0.3.
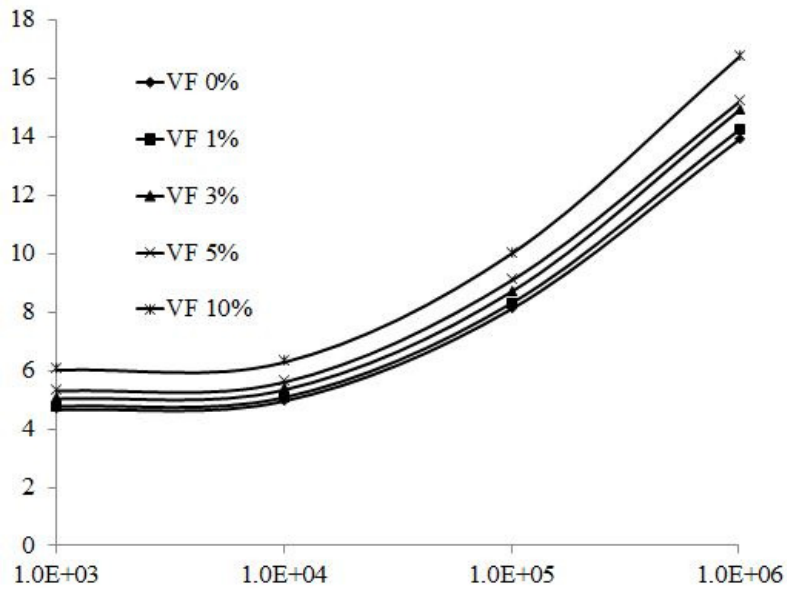
Figure 6: Average Nusselt number in inverse L-shaped of cavity for AR = 0.4.

Figure 7 Average Nusselt number in inverse L-shaped of cavity for AR = 0.4. 1%

Figure 8 Average Nusselt number in inverse L-shaped of cavity for AR = 0.4. 10%

5.0 CONCLUSIONS

The present commentary aimed at providing an in-depth discussion on the numerical methodology described in the work of He et al. [1]. The contribution of the present work is in correcting a number of mistakes made in an attempt to predict the heat and flow characteristics of nanofluids in enclosure. We recommend that the authors perform code validation by comparing with the well-known benchmark solution. We also suggest that the authors conduct

a grid independence test on the most critical condition of their research case in order to comprehend the effect of grid size on the numerical solution.

REFERENCES

[1]   He, Yurong, Cong Qi, Yanwei Hu, Bin Qin, Fengchen Li, and Yulong Ding. "Lattice Boltzmann simulation of alumina-water nanofluid in a square cavity." Nanoscale research letters 6, no. 1 (2011): 1-8.

[2]   Munir, F. A., N. A. C. Sidik, and Ibrahim NIN. "Numerical simulation of natural convection in an inclined square cavity." Journal of Applied Sciences 11, no. 2 (2011): 373-378.

[3]   Oueslati, Fakhreddine Segni, and Rachid Bennacer. "Heterogeneous nanofluids: natural convection heat transfer enhancement." Nanoscale research letters 6, no. 1 (2011): 1-11.

[4]   Azwadi, CS Nor, and M. S. Idris. "Finite different and lattice Boltzmann modelling for simulation of natural convection in a square cavity." International Journal of Mechanical and Materials Engineering 5, no. 1 (2010): 80-86.

[5]   Peng, Y., C. Shu, and Y. T. Chew. "Simplified thermal lattice Boltzmann model for incompressible thermal flows." Physical Review E 68, no. 2 (2003): 026701.

[6]   Sridhara, Veeranna, and Lakshmi Narayan Satapathy. "Al2O3-based nanofluids: a review." Nanoscale research letters 6, no. 1 (2011): 1-16.

[7]   Mahmoodi, Mostafa, and Seyed Mohammad Hashemi. "Numerical study of natural convection of a nanofluid in C-shaped enclosures." International Journal of Thermal Sciences 55 (2012): 76-89.

[8]   Heris, S. Zeinali, Seyyed Hossein Noie, Elham Talaii, and Javad Sargolzaei. "Numerical investigation of Al2O3/water nanofluid laminar convective heat transfer through triangular ducts." Nanoscale research letters 6, no. 1 (2011): 1.

[9]   Vadasz, Peter. "Heat transfer augmentation in nanofluids via nanofins." Nanoscale research letters 6, no. 1 (2011): 1-12.